# Theoretical Study of the Ionization of Phenol−Water and Phenol−Ammonia Hydrogen-Bonded Complexes

**Mariona Sodupe, Antonio Oliva, and Juan Bertrán***

*Departament de Química, Unitat de Química Física, Universitat Autònoma de Barcelona, 08193 Bellaterra, Barcelona, Spain*

*Received: February 14, 1997; In Final Form: June 2, 1997*[⊗]

The ionization of phenol−water and phenol−ammonia complexes have been determined both using ab initio methods that include electron correlation and the hybrid three-parameter B3LYP density functional method. The most stable structure of phenol−water cation corresponds to the $C_6H_5OH^+-H_2O$ non-proton-transferred complex. However, for the phenol−ammonia cation the calculations indicate that the only minimum on the potential energy surface corresponds to the $C_6H_5O-NH_4^+$ proton transferred form. The computed B3LYP adiabatic ionization potentials for $C_6H_5OH-H_2O$ and $C_6H_5OH-NH_3$ have been determined to be 7.65 and 7.33 eV, respectively. The results obtained indicate that, for the neutral H-bonded systems, the B3LYP density functional method yields very similar results to those obtained with the ab initio MP2 or MCPF methods. However, for the ionized radical cations, B3LYP results compare much better with experiment and to the MCPF method than UMP2. The unscaled B3LYP vibrational frequencies are in very good agreement with the known experimental data.

## Introduction

The development of ultrafast laser techniques with femtosecond resolution have made possible to study real-time molecular dynamic processes.[1] On the theoretical side, many dynamic studies are based on the knowledge of the potential energy surface. Because the direct inversion of the experimental spectra into a potential energy surface is intractable,[2] a close interaction between theory and experiment is required for obtaining a good understanding of the experimental results.

The study of ionic hydrogen bonded clusters involving phenol and simple molecules, such as water or ammonia, has attracted considerable attention as models for studying numerous biological and chemical processes.[3−14] One of the simplest and most fundamental chemical processes that can occur upon ionization is the proton-transfer reaction. Because of that, several experimental studies have investigated the size dependence intracluster proton-transfer reaction in $[phenol-(H_2O)_n]^+$ and $[phenol-(NH_3)_n]^+$. These studies have shown that for $[C_6H_5OH-(H_2O)_n]^+$ the proton-transfer reaction takes place for $n \geq 3$, while for $n = 1$ and $n = 2$ the most stable ion structure corresponds to the $C_6H_5OH^+-(H_2O)_n$ non-proton-transferred form.[13,14] However, for phenol$-NH_3$, the electronic spectra seems to indicate that the ground-state structure of the ion arises from the interaction of the phenoxyl radical and the ammonium ion; that is, it corresponds to the $C_6H_5O-NH_4^+$ proton transferred form.[12] For this system, an energy barrier of about 1 eV has been estimated for the proton-transfer reaction from $C_6H_5OH^+-NH_3$ to $C_6H_5O-NH_4^+$.[9−11] This large barrier has been suggested from two color picosecond excitation and delayed ionization from an excited neutral proton-transfer experiment. This is in contrast to the $H_2O-H_2O$ and $H_2O-NH_3$ dimers, for which ionization of the proton donor monomer spontaneously leads, in both cases, to the proton transferred structures $OH-H_3O^+$ and $OH-NH_4^+$, respectively.[15−17] This surprisingly large barrier for the proton-transfer reaction from $C_6H_5OH^+-NH_3$ to $C_6H_5O-NH_4^+$ has been attributed to the fact that the charge is very delocalized in the phenol fragment.[9]

Most of the previous theoretical studies for these systems deal with the neutral complexes.[18−23] To our knowledge, only one theoretical study has been performed for the $[C_6H_5OH-H_2O]^+$ radical cation.[24] However, in this study the geometry and only the low vibrational frequencies were determined at the restricted open Hartree−Fock (HF) level, without considering electron correlation in general and, in particular, spin polarization. Very recently, Scheiner et al.[25] published a theoretical study for the phenol−ammonia system in the ground and excited states, in which the ionized state was considered as well. In this study geometry optimizations were carried out under certain constraints with the unrestricted HF (UHF) method, again without including the effect of electron correlation. Single-point calculations, at the UHF geometries, were performed at the UMP2 level. No vibrational frequencies for this system have been reported.

It is well-known that correlation energy can change dramatically the topology of a potential energy surface. Moreover, Hartree−Fock frequencies are known to be too large. In this paper we optimize the structures and determine the vibrational frequencies of the neutral and cationic $[C_6H_5OH-H_2O]$ and $[C_6H_5OH-NH_3]$ complexes using traditional ab initio methods that include electron correlation and methods based on the density functional approach. We will show that the density functional approach provides very good results, especially for the radical cation complexes, at a lower computational cost than conventional ab initio correlated methods. Differences between the phenol−water and phenol−ammonia systems, as well as those with previous theoretical studies, will be discussed.

## Methods

The adequacy of density functional methods for the study of hydrogen bonded compounds has been the subject of several recent papers.[26−37] It is generally agreed that local density functional methods are seriously deficient, while nonlocal methods that include gradient corrections, in particular the hybrid three-parameter B3LYP method,[38] provide results comparable to the MP2 ones when similar basis sets are used.

Based on the comparison between conventional ab initio and density functional methods in a series of complexes, it is

[⊗] Abstract published in *Advance ACS Abstracts,* November 1, 1997.

S1089-5639(97)00571-9 CCC: $14.00 

concluded that presently functionals do not cover the dispersion energy,[39,40] while the electrostatic interaction is properly described. An extension of the density functional formalism to include long range interactions such as the dispersion forces has recently been presented.[41] Because the dispersion forces are a minor component in the hydrogen bond interaction, it is not surprising that the B3LYP method provides reliable results for the H-bonded systems.

Although for neutral hydrogen bonded compounds, the B3LYP and MP2 methods can provide similar accuracy, for ionized radical cations the B3LYP method has been shown to perform much better. In particular, for the methanol radical cation, Radom et al.[42] have shown that the MP2 method gives an artificially short C−O bond length due to an overestimation of the effects of hyperconjugation, while at the B3LYP level this effect is only slightly overestimated leading to results in much better agreement with high level CCSD(T)[42] and G2 methods.[43] Ventura et al.[44] have shown that the bad description of the $XHCO^+$ radical cations at the Hartree−Fock level leads to an oscillatory behavior of the MP*n* series. There are other examples in the literature in which the B3LYP method is shown to provide better results than MP2.[45−48] The failure of the MP2 method for these systems has mainly been attributed to the spin contamination of the UHF wave function, since it is well-known that the Møller−Plesset perturbation expansion converges slowly when the UHF reference wave function has large spin contamination.[49,50] Improved energies can be obtained by employing a projector formalism which annihilates the contamination of higher spins.[51] Møller Plesset calculations based on a spin restricted approach (ROMPn) avoid the spin contamination problem; however, the perturbation treatment is not unique and several schemes have been proposed.[52] In the density functional approach it is not quite clear what the meaning of spin contamination is, since the single determinant of Kohn Sham orbitals is not the exact wave function. Nevertheless, little spin contamination is found for stable open shell molecules with these methods.[53]

In this work the geometries of the neutral and cationic [$C_6H_5OH-H_2O$] and [$C_6H_5OH-NH_3$] complexes have been determined both using MP2 and the three-parameter hybrid B3LYP density functional method,[38] implemented in the Gaussian 94 package.[54] Single-point calculations, at the B3LYP equilibrium geometries, have been performed using the modified coupled pair MCPF method.[55] The MCPF method is an extension of the singles and doubles configuration interaction approach, which is essentially size extensive and accounts for the effect of higher than doubles excitations in an approximate manner. For a great number of systems, in particular for electrostatically bound ones, the MCPF method has been shown to provide reliable results similar to the CCSD(T) or QCISD(T) methods. MCPF calculations have been performed with the Sweden-MOLECULE system programs.[56] Single-point calculations at the MP4 level including singles, doubles, triples and quadruples excitations have also been performed at the MP2 geometries. In the MP*n* and MCPF calculations, we have correlated all the electrons except the 1s-like ones of C, N, and O. Open shell MCPF calculations are based on a spin restricted formalism while we used the unrestricted approach for the MP*n* and the B3LYP calculations.

Harmonic vibrational frequencies have only been determined at the B3LYP level. We have chosen the B3LYP density functional method since it has recently been shown to provide very accurate results for the phenol cation[57] and phenoxyl radicals.[58] In particular, the unscaled B3LYP vibrational frequencies were found to be more accurate than the uniformly scaled UMP2 derived frequencies.[57] Moreover, the calculated B3LYP proton affinity for the $PhO^\bullet$ radical was found to be in very good agreement with the experimental results.[57] A reliable theoretical determination of the proton affinity of $C_6H_5O^\bullet$ is important for obtaining a good description of the cationic [$C_6H_5OH-H_2O]^+$ and [$C_6H_5OH-NH_3]^+$ complexes, specially the latter, for which the proton transfer [$C_6H_5O-NH_4^+$] complex has been detected in the experiments.

B3LYP calculations were performed using a double-$\zeta$ plus polarization and diffuse functions quality basis set. For C, N, and O we used the (9s5p)/4s2p set developed by Dunning[59] supplemented with a valence diffuse function ($\alpha_{sp} = 0.0438$ for carbon, $\alpha_{sp} = 0.0639$ for nitrogen and $\alpha_{sp} = 0.0845$ for oxygen) and one 3d function ($\alpha = 0.75$ for carbon, $\alpha = 0.80$ for nitrogen and $\alpha = 0.85$ for oxygen). For hydrogen, the basis set used is the (4s)/2s set of Dunning supplemented with a diffuse function ($\alpha = 0.036$) and a p polarization function ($\alpha = 1.00$). This basis set will be referred to as D95++** in the paper. MP2 calculations have been performed using the somewhat smaller D95* basis set, derived from the previous one, in which the diffuse functions and the polarization functions on the hydrogen atoms have not been included. For the purpose of comparison, we have also performed calculations at the B3LYP level with the smaller basis set. Basis set superposition error has been corrected by using the somewhat controversial[60] counterpoise correction.[61]

## Results and Discussion

First, we will present the structure and vibrational frequencies for the neutral [$C_6H_5OH-H_2O$] and [$C_6H_5OH-NH_3$] complexes. Next, we will study the effect of ionization in the structure and vibrations of these complexes, and finally, we will discuss the observed differences.

**A. $C_6H_5OH-H_2O$ and $C_6H_5OH-NH_3$.** Phenol is more acidic than water or ammonia. Thus, the most stable structure for the hydrogen bonded $C_6H_5OH-H_2O$ and $C_6H_5OH-NH_3$ complexes is expected to have phenol acting as the proton donor and water or ammonia as the proton acceptor. Since previous theoretical studies[18−20] have found this structure as the most stable, we have only considered this isomer in the present work.

In Figure 1 we present the B3LYP(D95++**) and MP2-(D95*) optimized structures for the neutral and cationic phenol−water and phenol−ammonia complexes. For comparison we have also included the optimized geometries of neutral phenol, phenol cation, and the phenoxyl radical. We have not included the B3LYP(D95*)-optimized geometrical parameters since the obtained values are very similar to the ones obtained at the B3LYP level with the larger D95++** basis set. The most important differences correspond to the internuclear distances $O_7-O_{14}$ and $O_7-N_{14}$ of the neutral complexes, which are 0.028 and 0.030 Å smaller, respectively, in the D95* basis set. The differences between the MP2 and B3LYP values are also small. As it has been found in previous studies, B3LYP provides, in general, a somewhat smaller H-bond distance than the MP2 method.[35,39]

It can be observed in Figure 1 that both neutral complexes, $C_6H_5OH-H_2O$ (1d) and $C_6H_5OH-NH_3$ (1f), have $C_s$ symmetry with an almost linear hydrogen bond. Deviation from linearity is somewhat larger for phenol−ammonia than for phenol−water due to a stronger sterical interaction between ammonia and phenol. As expected, hydrogen-bonding interaction increases the $O_7-H_{13}$ bond distance of phenol, the lengthening being more important in $C_6H_5OH-NH_3$ than in $C_6H_5OH-H_2O$, due to the larger basicity of ammonia compared to that of water.

The internuclear distance *R* between the two heavy atoms is very similar in the two complexes, both at the B3LYP and MP2

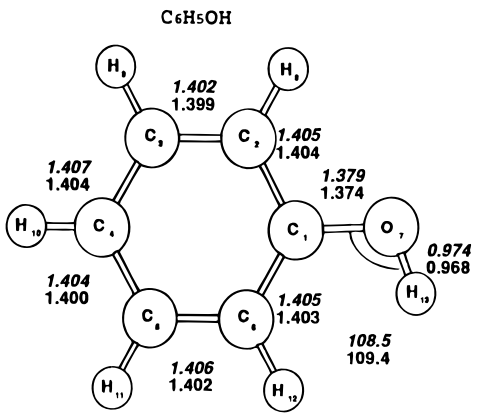
C6H5OH
1.402
1.399
1.405
1.404
1.379
1.374
1.407
1.404
0.974
0.968
1.404
1.400
1.405
1.403
108.5
109.4
1.406
1.402

a)

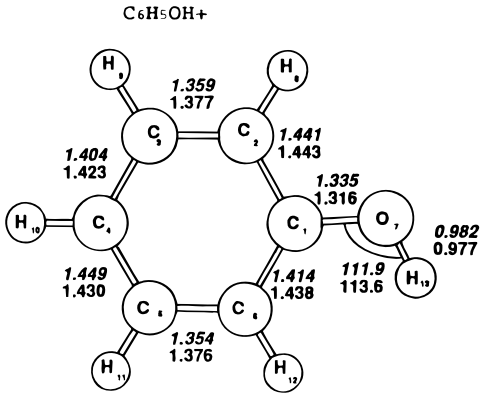
C6H5OH+
1.359
1.377
1.441
1.443
1.404
1.423
1.335
1.316
0.982
0.977
1.449
1.430
111.9
113.6
1.414
1.438
1.354
1.376

b)

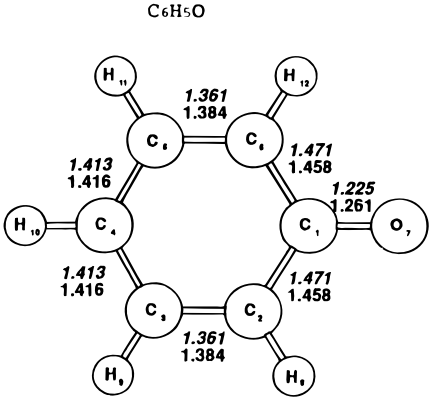
C6H5O
1.361
1.384
1.471
1.458
1.413
1.416
1.225
1.261
1.413
1.416
1.471
1.458
1.361
1.384

c)

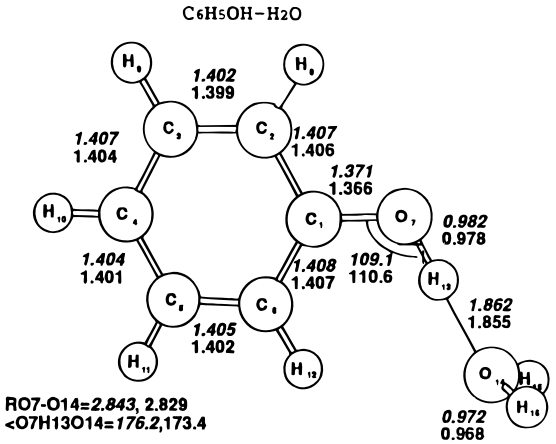
C6H5OH−H2O
1.402
1.399
1.407
1.404
1.407
1.406
1.371
1.366
0.982
0.978
1.404
1.401
1.408
1.407
109.1
110.6
1.862
1.855
1.405
1.402
RO7-O14=2.843, 2.829
<O7H13O14=176.2,173.4
0.972
0.968

d)

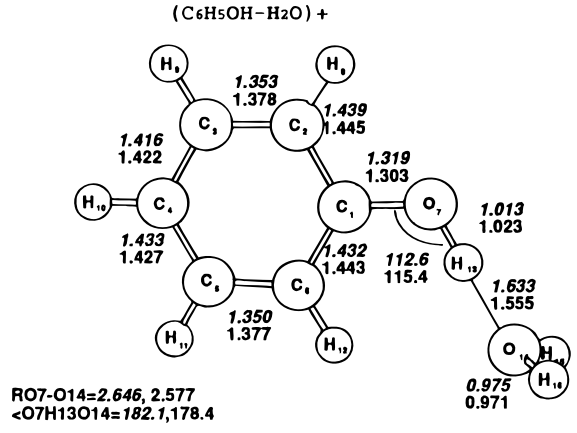
(C6H5OH−H2O)+
1.353
1.378
1.439
1.445
1.416
1.422
1.319
1.303
1.013
1.023
1.433
1.427
1.432
1.443
112.6
115.4
1.633
1.555
1.350
1.377
0.975
0.971
RO7-O14=2.646, 2.577
<O7H13O14=182.1,178.4

e)

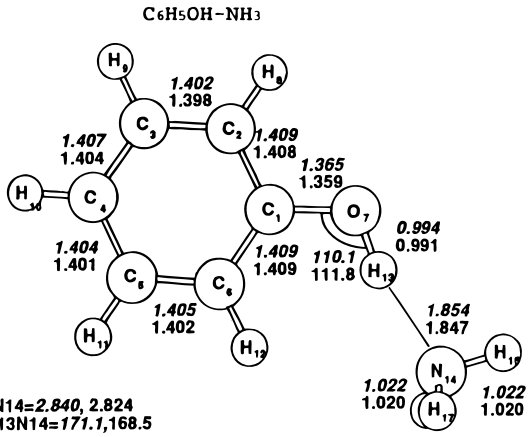
C6H5OH−NH3
1.402
1.398
1.407
1.404
1.409
1.408
1.365
1.359
0.994
0.991
1.404
1.401
1.409
1.409
110.1
111.8
1.854
1.847
1.405
1.402
1.022
1.020
1.022
1.020
RO7-N14=2.840, 2.824
<O7H13N14=171.1,168.5

f)

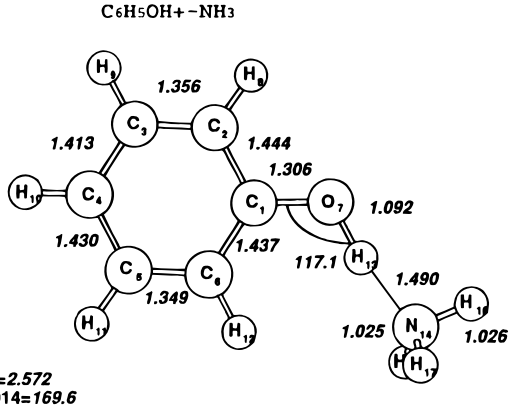
C6H5OH+−NH3
1.356
1.413
1.444
1.306
1.092
1.430
1.437
117.1
1.490
1.349
1.025
1.026
RO7-N14=2.572
<O7H13O14=169.6

g)

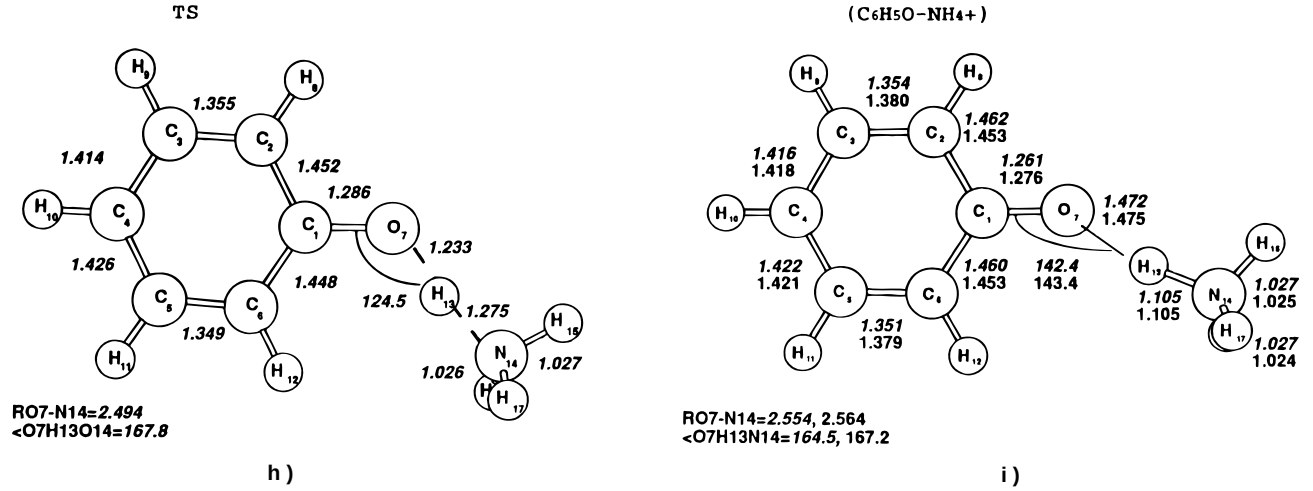


**Figure 1.** MP2- B3LYP-optimized geometries of (a) $C_6H_5OH$, (b) $C_6H_5OH^+$, (c) $C_6H_5O^{\bullet}$, (d) $C_6H_5OH-H_2O$, (e) $C_6H_5OH^+-H_2O$, (f) $C_6H_5OH-NH_3$, (g) $C_6H_5OH^+-NH_3$, (h) TS for the proton-transfer reaction $C_6H_5O-H^+-NH_3$, and (i) $C_6H_5O-NH_4^+$. Distances are in angstroms and angles in degrees.

**TABLE 1: Binding Energies of $C_6H_5OH$-$H_2O$ and $C_6H_5OH-NH_3$[a]**

| | $C_6H_5OH-H_2O$[b] | $C_6H_5OH-NH_3$[b] |
|---|---|---|
| MP2(D95*)//MP2(D95*) | 9.3(7.1) | 12.0(8.6) |
| MP4(D95*)//MP2(D95*) | 9.1 | 11.6 |
| B3LYP(D95*)//B3LYP(D95*) | 8.7(7.6) | 11.3(9.5) |
| MP2(D95++**)//MP2(D95*) | 9.0(6.1) | 11.0(8.1) |
| B3LYP(D95++**)//B3LYP(D95++**) | 7.5(6.4) | 9.7(8.6) |
| MCPF(D95++**)//B3LYP(D95++**) | 8.3 | 10.0 |

[a] In parentheses are counterpoise corrected binding energies. [b] In kcal/mol.

levels. This is consistent with the experimental value of $R$ in the $H_2O-H_2O$ and $H_2O-NH_3$ dimers, which has been determined to be 2.98 Å[62,63] in both complexes. However, previous Hartree−Fock calculations found the $R$ value to be about 0.05 Å larger in phenol−ammonia than in phenol−water.[22] Moreover, the HF value for the $R$ distance in both complexes is about 0.1 Å larger than the value obtained in the present work. These differences are due to fact that electron correlation is neglected in the HF studies while it is taken into account in the present calculations, which mainly changes the electronic charge distribution of the monomers and, thereby the electrostatic interaction. The obtained values of $R$ for $C_6H_5OH-H_2O$ at the B3LYP (2.83 Å) and at the MP2 (2.84 Å) levels are in better agreement with the experimental value of about 2.86 Å reported in ref 64 than with the 2.93 Å value determined in ref 65 by performing another analysis of the rotational constants. For the *trans*-1-naphtol−$NH_3$ complex, a value of 2.86 Å has been experimentally determined.[66]

The computed binding energies $D_e$ of $C_6H_5OH-H_2O$ and $C_6H_5OH-NH_3$, at different levels of calculation, are given in Table 1. The binding energies computed with the D95* basis are somewhat larger than the ones obtained with the D95++** basis set. As noted previously,[18] the counterpoise corrected binding energies should be taken with some reservation with basis sets containing diffuse functions, since the correction might be overestimated. The uncorrected B3LYP binding energies are slightly smaller than the values obtained with conventional ab initio methods, probably due to the fact that the dispersion energy is not covered with presently density functional methods.[39,40] However, the differences are small and the computed values are in good agreement with the ab initio values obtained with the MP2 and the high-level MCPF methods. Overall, the uncorrected B3LYP value with the large basis set can be quite accurate, since the basis set superposition error can partially compensate the lack of dispersion energy. The binding energy of $C_6H_5OH-H_2O$ at the B3LYP (7.5kcal/mol) and MCPF (8.3 kcal/mol) levels are also very close to the best estimate of 7.8 kcal/mol reported by Feller et al. at the MP2 level using large correlation consistent basis set.[18] Including the B3LYP zero-point correction, the B3LYP(MCPF) binding energies $D_0$ of phenol−water and phenol−ammonia are 5.6(6.4) and 7.8(8.1) kcal/mol, respectively. A larger binding energy for phenol−ammonia was to be expected considering that ammonia is a better proton acceptor than water.

The B3LYP vibrational frequencies of $C_6H_5OH-H_2O$ and $C_6H_5OH-NH_3$, as well as the shifts of the intramolecular modes of free phenol and water or ammonia, are given in Table 2. There are six intermolecular vibrations arising from the hydrogen bonding interaction between phenol and water or phenol and ammonia: two $a''$ rocking modes, two $a'$ wagging modes, one $a''$ torsional mode and the $a'$ hydrogen bonding stretch. As used by Schütz et al.,[19] the rocking modes are denoted $\tau_1$ and $\tau_2$, the wagging modes $\beta_1$ and $\beta_2$, the torsional mode t and the H-bond stretch $\sigma$. It has been previously noted that the anharmonic correction is important for the $\beta_2$ intermolecular wag mode of the phenol−water complex.[19] However, for the $C_6H_5OH-NH_3$ system the computed $\beta_2$ harmonic value is in very good agreement with the experimental one, which appears to indicate that in this case the anharmonic correction is not important. Moreover, the harmonic description was found to be very reasonable for the stretching mode $\sigma$ in both systems, as can be observed in Table 2. As found in experiments, this $\sigma$ H-bond stretch is larger in phenol−ammonia[21,22] than in phenol−water,[67,68] which is consistent with the larger binding interaction in $C_6H_5OH-NH_3$.

With respect to the intramolecular modes, it can be observed in Table 2 that the larger frequency shifts due to the hydrogen bonding interaction are those associated with the phenolic group OH, i.e., the $a''$ OH torsional mode and the $a'$ O−H stretching mode. The computed shifts of the O−H stretching mode in $C_6H_5OH-H_2O$ ($-208$ cm$^{-1}$) and $C_6H_5OH-NH_3$ ($-469$ cm$^{-1}$) are larger than the experimental values of $-134$ cm$^{-1}$ [69] and $-363$ cm$^{-1}$,[21] respectively. This overestimation is probably due to the fact that the computed $R$ distance in the complex at the B3LYP level might be slightly underestimated.[35]

The computed B3LYP frequencies, specially the low-frequency vibrations, are in very good agreement with the experimental data. Moreover, for phenol−ammonia, the NH

**TABLE 2: B3LYP Harmonic Vibrational Frequencies of the $C_6H_5OH-H_2O$ and $C_6H_5OH-NH_3$ Hydrogen Bonded Dimers and Frequency Shifts Compared to Free Monomers**

| | intermolecular vibrations | | |
|---|---|---|---|
| $C_6H_5OH-H_2O$[b] frequency | | $C_6H_5OH-NH_3$[c] frequency | |
| (a″) $\rho_1$ | 37 | (a″) $\rho_1$ | 38 |
| (a′) $\beta$1 | 58 | (a″) $\tau$ | 41 |
| (a″) $\tau$ | 88 | (a′) $\beta$1 | 66 (60) |
| (a′) $\sigma$ | 163 (151) | (a″) $\sigma$ | 188 (164) |
| (a″) $\rho$2 | 254 | (a″) $\rho$2 | 284 |
| (a′) $\beta$2 | 262 (146) | (a′) $\beta$2 | 322 (322) |

| | intramolecular vibrations | | | | |
|---|---|---|---|---|---|
| $C_6H_5OH-H_2O$[b] | frequency | shift | $C_6H_5OH-NH_3$[a] | frequency | shift |
| (a″) ring tors.[d] | 229 | +1 | (a″) ring tors. | 229 | +1 |
| (a″) ring. tors. | 421 | +5 | (a″) ring tors. | 417 | +1 |
| (a′) CO bend | 435 | +32 | (a′) CO bend | 464 | +61 |
| (a″) ring tors. | 517 | +6 | (a″) ring tors. | 514(525) | +3 |
| (a′) ring def. | 530 (528) | +1 | (a′) ring def. | 533 | +4 |
| (a′) ring def. | 624 (618) | +1 | (a′) ring def. | 624 | +1 |
| (a″) ring tors. | 697 | +14 | (a″) ring tors. | 684 | +1 |
| (a″) CH op bend | 759 | −3 | (a″) CH op bend | 761 | −1 |
| (a″) OH tors. | 775 | +447 | (a″) CH op bend | 825 | −2 |
| (a′) C−O str., ring def. | 825 (825) | +4 | (a′) C−O str., ring def. | 828 | +7 |
| (a″) CH op bend | 840 (813) | +13 | (a″) CH op bend | 888 | −7 |
| (a″) CH op bend | 901 | +6 | (a″) OH tors. | 902 (822) | +574 |
| (a″) CH op bend | 971 | +3 | (a″) CH op bend | 964 | −4 |
| (a″) CH op bend | 981 | −2 | (a″) CH op bend | 977 | −6 |
| (a′) ring def. | 998 (1000) | −1 | (a′) ring def. | 997 (996) | −2 |
| (a′) C−C str. | 1039 (1026) | 0 | (a′) C−C str. | 1038 (1025) | −1 |
| (a′) C−C str., CH ip bend | 1091 (1070) | +2 | (a′) C−C str., CH ip bend | 1090 | +1 |
| (a′) CH ip bend | 1171 (1151) | 0 | (a′) $NH_3$ inv. | 1130 | +115 |
| (a′) CH ip bend | 1183 | −2 | (a′) CH ip bend | 1170 | −1 |
| (a′) OH bend, C−C str., CH ip bend | 1243 | +62 | (a′) CH ip bend | 1181 | −4 |
| (a′) C−O str., C−C str. | 1293 (1274) | +14 | (a′) OH bend, C−C str., CH ip bend | 1275 | +94 |
| (a′) CH ip bend | 1356 | +4 | (a′) C−O str., C−C str. | 1301 (1279) | +22 |
| (a′) C−C str., OH bend, CH ip bend | 1383 | +18 | (a′) CH ip bend | 1356 | +4 |
| (a′) C−C str., CH ip bend | 1494 | +2 | (a′) C−C str., OH bend, CH ip bend | 1414 | +49 |
| (a′) C−C str., CH ip bend | 1525 | +4 | (a′) C−C str. CH ip bend | 1499 | +7 |
| (a′) $H_2O$ bend | 1624 | +25 | (a′) C−C str., CH ip bend | 1527 | +6 |
| (a′) C−C str. | 1634 | −4 | (a′) C−C str. | 1631 | −7 |
| (a′) C−C str. | 1652 | +1 | (a′) C−C str. | 1652 | +1 |
| (a′) C−H str. | 3174 (3032) | +8 | (a′) $NH_3$ bend | 1666 | −3 |
| (a′) C−H str. | 3180 (3054) | −4 | (a″) $NH_3$ bend | 1668 | −1 |
| (a′) C−H str. | 3191 (3072) | −1 | (a′) C−H str. | 3171 | +5 |
| (a′) C−H str. | 3201 | −5 | (a′) C−H str. | 3179 | −5 |
| (a′) C−H str. | 3209 (3087) | −5 | (a′) C−H str. | 3189 (3058) | −3 |
| (a′) O−H str. | 3632 (3524) | −208 | (a′) C−H str. | 3200 (3083) | −6 |
| (a′) $H_2O$ str. | 3817 (3650) | −3 | (a′) C−H str. | 3208 | −6 |
| (a″) $H_2O$ str. | 3930 (3748) | −11 | (a′) O−H str. | 3371 (3294) | −469 |
| | | | (a′) $NH_3$ str. | 3480 (3333) | −6 |
| | | | (a′) $NH_3$ str. | 3609 | −20 |
| | | | (a″) $NH_3$ str. | 3614 | −15 |

[a] Frequencies in $cm^{-1}$. Abbreviations: op = out-of-plane, ip = in-plane. Experimental values in parentheses. [b] Experimental values taken from refs 19, 67, 69, 70, and 72. [c] Experimental values taken from refs 21, 22, and 69. [d] Abbreviations for molecular motions: tors = torsional, def = deformational, and str = stretching,

and OH B3LYP stretching frequencies show the same ordering than that observed in the experiments,[21] that is, the frequency of the OH stretching vibration is lower than the NH stretching, while previous Hartree−Fock results, with double-$\zeta$ plus polarization quality basis sets, gave the reverse order.[21,22] The computed B3LYP frequencies of phenol are also in better agreement with experiment than the MP2 ones.[18] A very good agreement between the experimental and density functional results for the vibrational spectrum of phenol has also been recently reported by Michalska et al. using the BLYP method.[71]

**B. $C_6H_5OH-H_2O^+$ and $C_6H_5OH-NH_3^+$.** Phenol has a lower ionization potential than water or ammonia. Moreover, hydrogen bonding interaction lowers the energy required to ionize the proton donor molecule, due to a destabilization of the HOMO orbital of the donor monomer.[15−17] Thus, the lowest ionic state of phenol−water and phenol−ammonia is a $^2A''$ state derived from ionizing the phenol monomer.

Let us first consider the $[C_6H_5OH-H_2O]^+$ cation. The computed B3LYP (MCPF) vertical ionization potential of phenol−water is 7.93 eV (7.83), 0.53 (0.53) eV smaller than that of free phenol 8.46 (8.36) eV. Geometrical relaxation of the $^2A''$ state of $[C_6H_5OH-H_2O]^+$ leads to the non-proton-transferred structure displayed in Figure 1e. The most important geometrical change upon ionization corresponds to the $R_{O-O}$ hydrogen bond length, which decreases 0.197 (0.252) Å at the MP2(B3LYP) levels, mainly due to a stronger electrostatic interaction in the ion. Consequently, the increase of the $O_7-H_{13}$ bond length in the cation 0.031 (0.046) Å is significantly larger than in the neutral complex 0.008 (0.010) Å. The geometrical changes of the phenol fragment in the complex

**TABLE 3: Relative Energies (in kcal/mol) for the Ionized $(C_6H_5OH-H_2O)^+$ Complex**

| | $C_6H_5OH^+-H_2O$ | $C_6H_5O + H_3O^+$ |
|---|---|---|
| MP2(D95*)//MP2(D95*) | −22.6 (−20.0) | 49.4 |
| PMP2(D95*)//MP2(D95*)[b] | −24.8 | 33.1 |
| PMP2(D95*)//MP2(D95*)[c] | −24.4 | 37.8 |
| MP4(D95*)//MP2(D95*) | −22.5 | 45.2 |
| PMP4(D95*)//MP2(D95*)[b] | −24.4 | 31.4 |
| PMP4(D95*)//MP2(D95*)[c] | −24.0 | 35.8 |
| B3LYP(D95*)//B3LYP(D95*) | −24.2 (−23.0) | 38.7 |
| MP2(D95++**)//MP2(D95*) | −21.0 (−17.5) | 52.5 |
| PMP2(D95++**)//MP2(D95*)[b] | −23.3 | 36.3 |
| B3LYP(D95++**)//B3LYP(D95++**) | −21.6 (−20.3) | 41.6 |
| MCPF(D95++**)//B3LYP(D95++**) | −21.6 | 38.8 |

[a] In parentheses are counterpoise corrected energies. [b] Projected energies after annihilating the first contaminant (quartet). [c] Projected energies after annihilating all the contaminants from quartet to octet.

parallel those observed in the ionization of free phenol, see Figures 1a and 1b.

The relative energies of the $C_6H_5OH^+-H_2O$ cation computed with respect to the most stable $C_6H_5OH^+ + H_2O$ asymptote at different levels of calculation are given in Table 3. For comparison we have also included the relative energy of the proton transferred $C_6H_5O^\bullet + H_3O^+$ asymptote. Even though ionization increases the acidity of phenol, the most stable structure of phenol−water cation is the non-proton-transferred complex 1e. This is not surprising considering that the proton transferred $C_6H_5O^\bullet + H_3O^+$ asymptote lies high above the non-proton-transferred $C_6H_5OH^+ + H_2O$ one, that is, the B3LYP-(MCPF) proton affinity of $H_2O$ is 1.8 (1.7) eV smaller than that of the $C_6H_5O^\bullet$ radical. This is in contrast to the $(H_2O)_2$ dimer, for which ionization leads spontaneously to the proton transferred $OH-H_3O^+$ complex.[15] In that case, however, the $OH + H_3O^+$ asymptote lies about 1 eV below the $H_2O^+ + H_2O$ one, due to the larger proton affinity of $H_2O$ compared to that of OH.

It can be observed in Table 3 that, while the uncorrected relative energies of the $C_6H_5OH^+-H_2O$ complex are similar at all levels of calculations, that is, they do not differ by more than 2.5 kcal/mol within the same basis set, the differences in the relative energies of the $C_6H_5O^\bullet + H_3O^+$ asymptote can be as large as 18 kcal/mol. In particular, it can be observed that the MP2 energies are much too high compared with the B3LYP and the MCPF ones due to the high spin contamination of the phenoxyl radical. The value of $S^2$ in this system is 1.31, even larger than the values found in aromatic radical compounds, which are generally high-spin contaminated. Because of that, the MP2 energies are meaningless. Projected MP*n* energies are much closer to the B3LYP and MCPF results. The B3LYP and MCPF values, including the zero-point correction (0.01 kcal/mol), are very close to the experimental value of 40.6 kcal/mol obtained from the difference of the proton affinities of $C_6H_5O^\bullet$ and $H_2O$.[73,74] Therefore, it is clear from these results that the B3LYP method provides much better results than MP2 for these kind of systems. A better behavior of the less computationally demanding B3LYP method compared to MP2 has also been found by Morokuma et al. in the study of the decomposition of the phenoxyl radical cation.[75]

The computed $C_6H_5OH^+-H_2O$ binding energy $D_e$ both at the B3LYP and MCPF levels with the large basis set, is 21.6 kcal/mol. Including the zero-point correction, the binding energy is 19.6 kcal/mol. As expected, the binding energy in the cationic complex is significantly larger than in the neutral dimer, mainly due to a stronger electrostatic interaction in the cation. It can be observed that, at the B3LYP(MCPF) levels, the geometry relaxed $C_6H_5OH^+-H_2O$ complex (structure 1e) lies 6.4 (5.8) kcal/mol, 0.28 (0.25) eV, lower in energy than the vertical ionized $^2A''$ state, which leads to an adiabatic ionization potential of 7.65 (7.58) eV. The difference between the vertical and adiabatic ionization potentials of phenol−water is somewhat larger than that of phenol 0.19 (0.20) eV due to the reduction of the hydrogen bond length in the cationic complex, which further enhances the electrostatic interaction. The computed B3LYP(MCPF) adiabatic ionization potential, 7.65 (7.58) eV, is in good agreement with the experimental value of 7.94 eV.[4,6]

The B3LYP vibrational frequencies of the phenol−water cation are given in Table 4. We have also included the computed intramolecular shifts compared to free phenol cation and water. The observed differences between the frequencies of the neutral and cationic complexes reflect the strong increase of the interaction between phenol and water upon ionization. That is, the frequency of the stretch vibration $\sigma$ increases from 163 $cm^{-1}$ in the neutral complex to 255 $cm^{-1}$ in the cation. Moreover, those frequencies associated with the OH group of phenol exhibit larger shifts in the cation than in the neutral dimer. This is specially significant for the OH stretching of phenol, which shows a shift of −208 $cm^{-1}$ in the neutral, while the corresponding value in the cation is −875 $cm^{-1}$. The B3LYP computed frequencies are in very good agreement with the experimental values,[4] which again indicates the adequacy of this method for describing these radical cation systems. The largest low-frequency difference corresponds to the intermolecular in-plane wag mode $\beta_2$, which has been shown to be strongly anharmonic in a previous theoretical study.[24]

Let us now consider the $[C_6H_5OH-NH_3]^+$ complex. The B3LYP(MCPF) vertical ionization energy of phenol−ammonia is 7.79 (7.69) eV. As expected, complexation of phenol decreases the energy required to ionize phenol, the decrease being more important in phenol−ammonia, 0.67 (0.67) eV than in phenol−water, 0.53(0.53) eV. Geometry optimization of the $^2A''$ ionized state of $[C_6H_5OH-NH_3]^+$ leads to different structures depending on the method of calculation used. That is, at the MP2 level, the geometrical relaxation leads to the non-proton-transferred $C_6H_5OH^+-NH_3$ structure (Figure 1g), while with the B3LYP method, we obtained the proton transferred $C_6H_5O^\bullet-NH_4^+$ one (Figure 1i). Using B3LYP, we could not find a minimum corresponding to the non-proton-transferred isomer. Any attempt to optimize such an structure collapsed to the $C_6H_5O^\bullet-NH_4^+$ isomer. However, both the proton and non-proton-transferred structures were found as minima of the potential energy surface when using the MP2 method. The MP2 transition state connecting both minima has also been located and is shown in Figure 1h.

Similarly to the $C_6H_5OH^+$-$H_2O$ radical cation, the $R_{O-N}$ distance in the non-proton-transferred form $C_6H_5OH^+-NH_3$ decreases 0.268 Å upon ionization and the geometrical changes of the phenol fragment are similar to those found when ionizing free phenol. The proton transferred $C_6H_5O^\bullet-NH_4^+$ form arises from the interaction of $C_6H_5O^\bullet$ and $NH_4^+$ and thus, the geometrical parameters are similar to those of free $C_6H_5O^\bullet$ and $NH_4^+$. In particular, the $C_1-O_7$ distance in the proton transferred complex is smaller than in the non-proton-transferred form, as it is in the phenoxyl radical compared to that in the phenol radical cation, due to an increase of the $C_1-O_7$ double-bond character. A comparison of the geometrical parameters of $C_6H_5O^\bullet-NH_4^+$ with those of free $C_6H_5O^\bullet$ and $NH_4^+$, at the MP2(B3LYP) levels, shows that the most important geometrical change upon complexation corresponds to the $C_1-O_7$ distance in the phenoxyl radical, which increases 0.036 (0.015) Å, and

**TABLE 4: B3LYP Harmonic Vibrational Frequencies of the $C_6H_5OH$-$H_2O^+$ and $C_6H_5O-NH_4^+$ Hydrogen-Bonded Dimers and Frequency Shifts Compared to Free Monomers**

| | intermolecular vibrations | | |
|---|---|---|---|
| | $C_6H_5OH^+-H_2O$[b] frequency | | $C_6H_5O-NH_4^+$ frequency |
| (a″) $\rho_1$ | 73 (67) | (a″) $\rho_1$ | 18 |
| (a′) $\beta$1 | 85 (84) | (a′) $\beta$1 | 54 |
| (a″) $\tau$ | 156 ($\approx$130) | (a″) $\tau$ | 63 |
| (a′) $\sigma$ | 255 (240) | (a′) $\sigma$ | 266 |
| (a′) $\beta$2 | 395 (328) | (a′) $\beta$2 | 400 |
| (a″) $\rho$2 | 429 | (a″) $\rho$2 | 436 |

| | intramolecular vibrations | | | | |
|---|---|---|---|---|---|
| $C_6H_5OH^+-H_2O$[b] | frequency | shift | $C_6H_5O-NH_4^+$ | frequency | shift |
| (a″) ring tors.[c] | 200 (189) | +18 | (a″) ring tors. | 203 | +16 |
| (a″) ring. tors. | 366 (354) | +8 | (a″) ring tors. | 371 | −4 |
| (a″) ring tors. | 448 | +22 | (a″) ring tors. | 469 | −5 |
| (a′) CO bend | 471 (450) | +59 | (a′) CO bend | 480 | +38 |
| (a′) ring def. | 523 (516) | +4 | (a′) ring def. | 557 | +33 |
| (a′) ring def. | 573 | +11 | (a′) ring def. | 587 | −4 |
| (a″) ring tors. | 633 (636) | +14 | (a″) ring tors. | 646 | −6 |
| (a″) CH op bend | 798 | +6 | (a″) CH op bend | 795 | −5 |
| (a″) CH op bend | 805 | +1 | (a″) CH op bend | 816 | +19 |
| (a′) C−O str., ring def. | 817 (812) | +4 | (a′) C−O str., ring def. | 823 | +20 |
| (a″) CH op bend | 945 | +6 | (a″)CH op bend | 938 | +17 |
| (a′) ring def. | 980 (977) | −1 | (a′) ring def. | 978 | +8 |
| (a′) C−C str. | 994 | +5 | (a″) CH op bend | 995 | +15 |
| (a″) CH op bend | 1001 | +5 | (a′) C−C str. | 1001 | −5 |
| (a″) CH op bend | 1006 | +3 | (a″) CH op bend | 1007 | +21 |
| (a′) CH ip bend | 1103 | +6 | (a′) CH ip bend | 1098 | +12 |
| (a′) CH ip bend | 1163 | +25 | (a′) CH ip bend | 1165 | +5 |
| (a″) OH tors. | 1168 | +563 | (a′) CH ip bend | 1180 | +21 |
| (a′) CH ip bend | 1193 | −5 | (a′) CH ip bend | 1293 | +17 |
| (a′) CH ip bend, OH bend | 1259 | +76 | (a′) CH ip bend | 1368 | +24 |
| (a′) CH ip bend | 1372 | +17 | (a′) $NH_4^+$ def. | 1385 | −101 |
| (a′) C−O str., CH ip bend | 1399 | +12 | (a′) C−O str., CH ip bend | 1416 | +2 |
| (a′) CH ip bend, C−C str. | 1413 | +3 | (a′) CH ip bend, C−C str. | 1436 | −1 |
| (a′) C−C str., OH bend | 1467 | +25 | (a′) C−O str., CH ip bend | 1529 | +44 |
| (a′) C−O str., CH ip bend | 1520 | +18 | (a′) CH ip bend, $NH_4^+$ def. | 1540 | −3 |
| (a′) C−C str., CH ip bend | 1539 | +4 | (a′) $NH_4^+$ def., CH ip bend | 1544 | +58 |
| (a′) $H_2O$ bend | 1646 | +47 | (a″) $NH_4^+$ def. | 1560 | +74 |
| (a′) C−C str. | 1651 | −6 | (a′) C−C str. | 1610 | +25 |
| (a′)O−H str. | 2855 | −875 | (a′) $NH_4^+$ def. | 1725 | +4 |
| (a′) C−H str. | 3213 | +7 | (a″) $NH_4^+$ def. | 1729 | +8 |
| (a′) C−H str. | 3218 | −2 | (a′) $H_{bond}-NH_3$ str. | 2222 | −1156 |
| (a′) C−H str. | 3224 | −4 | (a′) CH str. | 3202 | +15 |
| (a′) C−H str. | 3230 | +7 | (a′) CH str. | 3209 | +15 |
| (a′) C−H str. | 3235 | −4 | (a′) CH str. | 3216 | +9 |
| (a′) $H_2O$str. | 3790 | −30 | (a′) CH str. | 3222 | +6 |
| (a″) $H_2O$ str. | 3889 | −52 | (a′) CH str. | 3229 | +10 |
| | | | (a′) $NH_4^+$ str. | 3450 | −52 |
| | | | (a′) $NH_4^+$ str. | 3554 | +52 |
| | | | (a″) $NH_4^+$ str. | 3560 | +58 |

[a] Frequencies in $cm^{-1}$. Experimental values in parentheses. Abbreviations: op = out-of-plane, ip = in-plane. [b] Experimental values taken from ref 4. [c] Abbreviations for molecular motions: tors = torsional, def = deformational, and str = stretching.

to the $H_{13}-N_{14}$ bond distance in $NH_4^+$, which increases 0.074 (0.076) Å. The internuclear *R* distance between the two heavy atoms is very similar to that found for the non-proton-transferred structure. In contrast to the other H-bonded dimers, in this structure the $R_{O-N}$ B3LYP distance is somewhat larger than the MP2 one. The geometrical values of the transition state of the proton-transfer reaction are intermediate between the proton and non-proton-transferred structures, while the $O_7-N_{14}$ distance is shorter.

The relative energies with respect to the most stable $C_6H_5OH^+ + NH_3$ asymptote, at different levels of calculations, are given in Table 5. Experimental values show that the proton affinity of $C_6H_5O$ (205.6 kcal/mol)[73] is very similar to that of $NH_3$(208.3kcal/mol).[76] Therefore, the non-proton-transferred $C_6H_5OH^+ + NH_3$ and the proton-ransferred $C_6H_5O^\bullet + NH_4^+$ asymptotes are now almost degenerate, i.e., the proton-transferred asymptote is slightly lower (−2.7 kcal/mol) than the non-proton-transferred one. It can be observed in Table 5 that the B3LYP(MCPF) relative energies of $C_6H_5O^\bullet + NH_4^+$, including the zero point correction (1.1 kcal/mol), are in good agreement with the experimental value. Again the MP2 results are too high due to the high-spin contamination of the unrestricted wave function of the phenoxyl radical. Consequently, the MP2 interaction energies of the proton transferred complex $C_6H_5O^\bullet-NH_4^+$ are 4−5 kcal/mol smaller than the B3LYP or MCPF values. In contrast, projected MP2 interaction energies, obtained after spin annihilation of the first contaminant (quartet), are larger by about 4−5 kcal/mol. The results with the small basis set show that the projected MP*n* energies and the B3LYP results become much closer when the remaining spin contaminants (sextet and octet) are projected out. In any case, all the projected energies increase the stability of the proton transferred $C_6H_5O^\bullet-NH_4^+$ structure with respect to the non-proton-transferred $C_6H_5OH^+-NH_3$ one, while the energy of the

**TABLE 5: Relative Energies (in kcal/mol) for the Ionized $(C_6H_5OH-NH_3)^+$ Complex[a]**

| | $C_6H_5OH^+-NH_3$ | TS | $C_6H_5O-NH_4^+$ | $C_6H_5O + NH_4^+$ |
|---|---|---|---|---|
| MP2(D95*)//MP2(D95*) | −28.5 (−24.2) | −28.2 | −28.8 (−26.7) | 7.1 |
| PMP2(D95*)//MP2(D95*)[b] | −32.7 | −34.8 | −38.0 | −9.1 |
| PMP2(D95*)//MP2(D95*)[c] | −31.9 | −33.3 | −35.8 | −4.3 |
| MP4(D95*)//MP2(D95*) | −28.2 | −28.0 | −29.9 | 3.0 |
| PMP4(D95*)//MP2(D95*))[b] | −31.6 | −33.5 | −37.5 | −10.8 |
| PMP4(D95*)//MP2(D95*))[c] | −30.8 | −32.2 | −35.5 | −6.3 |
| B3LYP(D95*)//B3LYP(D95*) | | | −33.1 (−32.2) | −2.3 |
| MP2(D95++**)//MP2(D95*) | −26.6 (−22.8) | −26.3 | −26.6 (−24.3) | 10.9 |
| PMP2(D95++**)//MP2(D95*)[b] | −30.8 | −32.9 | −35.6 | −5.2 |
| B3LYP(D95++**)//B3LYP(D95++**) | | | −31.3 (−30.7) | 0.9 |
| MCPF(D95++**)//B3LYP(D95++**) | | | −31.7 | −2.7 |

[a] In parentheses are counterpoise corrected energies. [b] Projected energies after annihilating the first contaminant (quartet). [c] Projected energies after annihilating all the contaminants from quartet to octet.

transition state becomes lower than that of the reactant. Thus, the energy barrier disappears after annihilating the spin contaminants, changing dramatically the topology of the potential energy surface. Moreover, the counterpoise correction shows that basis set superposition error is larger in $C_6H_5OH^+-NH_3$ than in $C_6H_5O^\bullet-NH_4^+$, which further increases the exothermicity of the reaction. Therefore, these results seem to indicate that the $C_6H_5OH^+-NH_3$ minimum at the MP2 level is an artifact of the method and of the basis set superposition error and that the only minimum on the potential energy surface is the proton transferred structure, as it is obtained at the B3LYP level.

Because the two asymptotes are almost degenerate, and considering that the electrostatic interaction is larger between $C_6H_5O^\bullet$ and $NH_4^+$ than between $C_6H_5OH^+$ and $NH_3$, due to fact that the charge is more localized in the first case, it is not surprising that the proton transferred $C_6H_5O^\bullet-NH_4^+$ complex is the most stable structure for the phenol−ammonia radical cation. The present results are in good agreement with the trapped ion photodissociation spectroscopy results which show that the ground-state ion of phenol−ammonia consists of a phenoxyl radical interacting with the ammonium ion.[12] However, while the experimental studies have estimated a barrier of about 1 eV between the non-proton-transferred and the proton-transferred complexes,[9−11] our results seem to indicate that $C_6H_5O^\bullet-NH_4^+$ is the only minimum on the potential energy surface. This large barrier was suggested because the phenol−ammonia cation did not undergo dissociative proton transfer to $C_6H_5O + NH_4^+$ at energies up to and exceeding 1 eV above the ion minimum. The nonobservation of $NH_4^+$ implied either the presence of a large barrier for the proton-transfer reaction or the formation of a very stable proton transferred $C_6H_5O-NH_4^+$ complex that does not easily dissociate. It can be observed in Table 5 that the B3LYP(MCPF) binding energy $D_e$ of the $C_6H_5O-NH_4^+$ complex, with respect to the $C_6H_5O + NH_4^+$ asymptote, is 32.2 (29.0) kcal/mol, that is, a very stable phenoxylammonium complex is formed upon ionization. However, this large stability would not explain why the nonproton-transferred fragments were observed in the experiments and not the proton transferred ones, given that both asymptotes are nearly at the same energy. Although the presence of a large barrier would be a reasonable explanation of the experimental results, our theoretical study and that of Scheiner et al.[25] do not support this hypothesis at all. Moreover, a large barrier for this proton-transfer reaction would be surprising considering the short H-bond *R* distance in the complex.

The main reason invoked to explain the appearance of this high barrier is that the charge, initially delocalized in the reactant, needs to localize for the proton transfer to occur.[9] However, Mulliken population at the MP2(D95*) geometries of the reactant, product and transition state, shows that the positive charge is mainly localized on the hydrogen atom that is transferred and that it remains almost constant along the process, that is, the $H_{13}$ atomic charge is 0.56 in the reactant, 0.52 in the transition state, and 0.49 in the product. The proton-transfer process implies an electron transfer in the opposite direction, which produces a decrease of the positive charge in the donor fragment ($C_6H_5O$) from 0.30 in the reactant to 0.11 in the product. Finally, it must be pointed out that the proton transferred product is a distonic radical cation since the positive charge and the spin are localized in different fragments.

The interpretation of the experimental results would, thus, require a theoretical dynamic study of the initial wave packet. This study is specially difficult because the proton-transfer reaction cannot be represented by a bidimensional potential energy surface, since important geometrical changes occur after ionizing the $C_6H_5OH-NH_3$ complex, in addition to those associated to the two variables ($O_7-N_{14}$ and $O_7-H_{13}$) directly involved in the proton-transfer process. In particular, there is an important decrease of the $C_1-O_7$ distance due to the increase of its double-bond character. Also, the geometry of the $C_6H_5$ ring changes from that of an aromatic ring, i.e., all the C−C distances are very similar, to that of a structure with an important quinoidal character, in which the $C_2-C_3$ and $C_5-C_6$ distances are much shorter than that of the other C−C bonds. Therefore, more than two dimensions need to be considered in a dynamical study. At present, this dynamical study is practically impossible in a so high multidimensional potential energy surface.

The phenoxylammonium structure, at the B3LYP(MCPF) levels, is 0.46 (0.48) eV more stable than the $^2A''$ vertical ionized state of $[C_6H_5OH-NH_3]^+$. Thus, the computed B3LYP(MCPF) adiabatic ionization potential is 7.33 (7.21) eV. The obtained results are in good agreement with the experimental results, which found that the ionization threshold of the complex lies at about 7.71[12] or 7.85 eV.[7,8] These experimental values correspond to the vertical ionization potential and thus, constitute an upper limit to the adiabatic ionization potential.

The vibrational frequencies of the $C_6H_5O-NH_4^+$ cation, as well as the shifts computed with respect to the isolated $C_6H_5O$ and $NH_4^+$ monomers, are given in Table 4. In this case the most important shifts correspond to those vibrations associated with the $NH_4^+$ monomer. In particular, $C_6H_5O-NH_4^+$ complexation produces a strong shift of the NH stretching involved in the hydrogen bond. On the basis of the good agreement between the B3LYP[58] and experimental frequencies of the phenoxyl radical, we also expect the computed frequencies of the cationic $C_6H_5O-NH_4^+$ complex to be accurate. Unfortunately, to our knowledge, no experimental vibrational frequencies for this complex have been reported.

## Conclusions

The ionization of phenol−water and phenol−ammonia complexes have been determined both using ab initio methods that

include electron correlation and using the hybrid three-parameter B3LYP density functional method. In both cases, the lowest ionic $^2A''$ state arises from ionizing the proton donor (phenol) molecule. However, while for the phenol−water cation, geometrical relaxation leads to a non-proton-transferred $C_6H_5OH^+-H_2O$ complex, for the phenol−ammonia cation the most stable structure corresponds to the proton-transferred $C_6H_5O-NH_4^+$ one. Our calculations seem to indicate that in this latter case the proton-transfer reaction takes place spontaneously, without any barrier, in contrast to the explanation given to the experimental results which assume a proton-transfer energy barrier of about 1 eV.[9−11]

The results obtained at different levels of calculation indicate that, for the neutral H-bonded systems, the B3LYP density functional method yields very similar results to those obtained with the ab initio MP2 or MCPF methods. However, for the ionized radical cations, B3LYP results compare much better with experiment and to the MCPF method than UMP2, due to the high-spin contamination in the UMP2 calculations. The good performance of B3LYP method for studying this kind of systems is encouraging, since the lower computational cost of B3LYP, compared to traditional ab initio correlated methods, allows the use of larger basis sets, which ultimately determines the accuracy of the results.

The unscaled B3LYP vibrational frequencies are also in very good agreement with the known experimental data. We expect that the present results will help in the assignment of the vibrational spectra of these complexes. A close interaction between theoreticians and experimentalists is desirable to interpret the fascinating experimental results that ultrafast laser techniques are providing.

**Acknowledgment.** Financial support from DGICYT through the PB92-0621 project and the use of the computational facilities of the Catalonia Supercomputer Center are gratefully acknowledged. We would also like to thank J. M. Lluch for helpful discussions.

## References and Notes

(1) Zewail, A. H. *J. Phys. Chem.* **1996**, *100*, 12701 and references therein.
(2) Bacic, Z.; Miller, R. E. *J. Phys. Chem*. **1996**, *100*, 12945.
(3) Brutschy, B. *Chem. Rev*. **1992**, *92*, 1567.
(4) Dopfer, O.; Reiser, G.; Müller-Dethlefs, K.; Schlag, E. W.; Colson, S. D. *J. Chem. Phys*. **1994**, *101*, 974.
(5) Dopfer, O.; Müller-Dethlefs, K. *J. Chem. Phys*. **1994**, *101*, 8508.
(6) (a) Lipert, R. J.; Colson, S. D. *J. Chem. Phys*. **1990**, *92*, 3240. (b) Lipert, R. J.; Colson, S. D. *J. Chem. Phys.* **1988**, *89*, 4579.
(7) Solgadi, D.; Jouvet, C.; Tramer, A. *J. Phys. Chem*. **1988**, *92*, 3313.
(8) Jouvet, C.; Lardeux-Dedonder, C.; Richard-Viard, M.; Solgadi, D.; Tramer, A. *J. Phys. Chem.* **1990**, *94*, 5041.
(9) Steadman, J.; Syage, J. A. *J. Am. Chem. Soc*. **1991**, *113*, 6786.
(10) Syage, J. A.; Steadman, J. *J. Phys. Chem*. **1992**, *96*, 9606.
(11) Mikami, N.; Okabe, A.; Suzuki, I *J. Phys. Chem*. **1988**, *92*, 1858.
(12) Mikami, N.; Sato, S.; Ishigaki, M. *Chem. Phys. Lett*. **1993**, *202*, 431.
(13) Sawamura, T.; Fujii, A.; Sato, S.; Ebata, T.; Mikami, N. *J. Phys. Chem*. **1996**, *100*, 8131.
(14) Sato, S.; Mikami, N. *J. Phys. Chem*. **1996**, *100*, 4765.
(15) Sodupe, M.; Oliva, A.; Bertran, J. *J. Am. Chem. Soc*. **1994**, *116*, 8249.
(16) Sodupe, M.; Oliva, A.; Bertran, J. *J. Am. Chem. Soc*. **1995**, *117*, 8416.
(17) Tomoda, S. *Faraday Discuss.* **1988**, *85*, 53.
(18) Feller, D.; Feyereisen, M. W. *J. Comput. Chem*. **1993**, *14*, 1027.
(19) Schütz, M.; Bürgi, T.; Leutwyler, S.; Fischer, T. *J. Chem. Phys*. **1993**, *98*, 3763.
(20) Watanabe, H.; Iwata, S. *J. Chem. Phys*. **1996**, *105*, 420.
(21) Iwasaki, A.; Fujii, A.; Watanabe, T.; Ebata, T.; Mikami, N. *J. Phys. Chem*. **1996**, *100*, 16053.
(22) Shiefke, A.; Deusen, C.; Jacoby, C.; Gerhards, M.; Schmitt, M.; Kleinermanns, K.; Hering, P. *J. Chem. Phys*. **1995**, *102*, 9197.
(23) Siebrand, W.; Zgierski, M. Z.; Smedarchina, Z. K.; Vener, M.; Kaneti, J. *Chem. Phys. Lett.* **1997**, *266*, 47.
(24) Hobza, P.; Burcl, R.; Spirko, V.; Dopfer, O.; Müller-Dethlefs, K.; Schlag, E. W. *J. Chem. Phys.* **1994**, *101*, 990.
(25) Yi M.; Scheiner, S. *Chem. Phys. Lett*. **1996**, *262*, 567.
(26) Novoa, J. J.; Sosa, C. *J. Phys. Chem*. **1995**, *99*, 15837.
(27) Lee, C.; Fitzgerald, G.; Planas, M.; Novoa, J. J. *J. Phys. Chem*. **1996**, *100*, 7398.
(28) Lee, C.; Sosa, C.; Planas, M.; Novoa, J. J. *J. Chem. Phys*. **1996**, *104*, 7081
(29) Sim, F.; St-Amant, A.; Papai, I.; Salahub, D. R. *J. Am. Chem. Soc*. **1992**, *114*, 4391.
(30) Wei, D.; Salahub, D. R. *J. Chem. Phys*. **1994**, *101*, 7633.
(31) Del Bene, J. E.; Person, W. B.; Szczepaniak, K. *J. Phys. Chem*. **1995**, *99*, 10705.
(32) Kieninger, M.; Suhai, S. *Int. J. Quantum Chem*. **1994**, *52*, 465.
(33) Gonzalez, L.; Mo, O.; Yañez, M.; Elguero, J. *J. Mol. Struct. (THEOCHEM)* **1996**, *371*, 1.
(34) Latajka, Z.; Bouteiller, Y.; Scheiner, S. *Chem. Phys. Lett*. **1995**, *234*, 159.
(35) Latajka, Z.; Bouteiller, Y. *J. Chem. Phys*. **1994**, *101*, 9793.
(36) Kim, K.; Jordan, K. D. *J. Phys. Chem*. **1994**, *98*, 10089.
(37) Alfredsson, M.; Ojamäe, L.; Hermansson, K. G. *Int. J. Quantum. Chem*. **1996**, *60*, 767.
(38) Becke, A. D. *J. Chem. Phys.* **1993**, *98*, 5648.
(39) Hobza, P.; Sponer, J.; Reschel, T.; *J. Comput. Chem*. **1995**, *16*, 1315.
(40) Kristyán, S.; Pulay, P. *Chem. Phys. Lett*. **1994**, *229*, 175.
(41) Lundqvist, B. I.; Andersson, Y.; Shao, H.; Chan, S.; Langreth, D. C. *Int. J. Quantum. Chem*. **1995**, *56*, 247.
(42) Gauld, J. W.; Glukhovtsev, M. N.; Radom, L. *Chem. Phys. Lett*. **1996**, *262*, 187.
(43) Wiest, O. *J. Mol. Struct. (THEOCHEM)* **1996**, *368*, 39.
(44) Ventura, O. N.; Kieninger, M.; Coitiño, E. L. *J. Comput. Chem*. **1996**, *17*, 1309.
(45) Barone, V.; Adamo, C. *Chem. Phys. Lett*. **1994**, *224*, 432.
(46) Barone V. *Theor. Chim. Acta* **1995**, *91*, 113.
(47) Zuilhof, H.; Dinnocenzo, J. P.; Chandrasekhar, A.; Shaik, S. *J. Phys. Chem*. **1996**, *100*, 15774.
(48) Baker, J.; Muir, M.; Andzelm, J. *J. Chem. Phys*. **1995**, *102*, 2063.
(49) Handy, N. C.; Knowles, P. J.; Somasundran, K. *Theor. Chim. Acta*. **1985**, *68*, 87.
(50) Tozer, D. J.; Handy, N. C.; Amos, R. D.; Pople, J. A.; Nobes, R. H.; Yaoming, X.; Schaefer, H. F. *Mol. Phys*. **1993**, *79*, 777
(51) Schlegel, H. B. *J. Chem. Phys.* **1986**, *84*, 4530.
(52) (a) Amos, R. D.; Andrews, J. S.; Handy, N. C.; Knowles, P. J. *Chem. Phys. Lett.* **1991**, *185*, 256. (b) Knowles, P. J.; Andrews J. S.; Amos, R. D.; Handy, N. C.; Pople, J. A. *Chem. Phys. Lett.* **1991**, *186*, 130. (c) Lauderdale, W. J.; Stanton, J. F.; Gauss, J.; Watts, J. D.; Bartlett, R. J. *Chem. Phys. Lett*. **1991**, *187*, 451. (d) Murray, C.; Davidson, E. R. *Chem. Phys. Lett.* **1991**, *187*, 451. (e) Lee, T. J.; Jayatilaka, D. *Chem. Phys. Lett*. **1993**, *201*, 1.
(53) (a)Baker, J.; Scheiner, A.; Andzelm, J. *Chem. Phys. Lett.* **1993**, *216*, 380. (b)Laming, G. J.; Handy, N. C.; Amos, R. D. *Mol. Phys*. **1993**, *80*, 1121.
(54) Frisch, M. J.; Trucks, G. W.; Schlegel, H. B; Gill, P. M. W.; Johnson, B. G.; Robb, M. A.; Cheeseman, J. R.; Keith, T.; Petersson, G. A.; Montgomery, J. A.; Raghavachari, K.; Al-Laham, M. A.; Zakrzewski, V. G.; Ortiz, J. V.; Foresman, J. B.; Peng, C. Y.; Ayala, P. Y.; Chen, W.; Wong, M. W.; Andres, J. L.; Replogle, E. S.; Gomperts, R.; Martin, R. L.; Fox, D. J.; Binkley, J. S.; Defrees, D. J.; Baker, J.; Stewart, J. P.; Head-Gordon, M.; Gonzalez, C. J. A. Pople, *Gaussian 94, Revision B.3*; Gaussian, Inc.: Pittsburgh, PA, 1995.
(55) Chong, D. P.; Langhoff, S. R. *J. Chem. Phys.* **1986**, *84*, 5606. Also see: Ahlrichs, R.; Scharf, P.; Ehrhardt, C. *J. Chem. Phys.* **1985**, *82*, 890.
(56) Sweden-MOLECULE is an electronic structure structure program written by J. Almlöf, C. W. Bauschlicher, M. R. A. Blomberg, D. P. Chong, A. Heiberg, S. R. Langhoff, P.-Å. Malmqvist, A. P. Rendell, B. O. Roos, P. E. M. Siegbahn and P. R. Taylor.
(57) Qin, Y.; Wheeler, R. A. *J. Phys. Chem.* **1996**, *100*, 10554.
(58) Qin, Y.; Wheeler, R. A. *J. Chem. Phys*. **1995**, *102*, 1689.
(59) Dunning, T. H., Jr.; Hay, P. *Modern Theoretical Chemistry*; Schaefer, H. F., III, Ed.; Plenum: New York, **1976**, 1−28.
(60) (a)Schwenke, D. W.; Truhlar, D. G. *J. Chem. Phys*. **1984**, *82*, 2418. (b) Frisch, M. J.; Del Bene, J. E.; Binkley, J. S.; Schaefer, H. F., III *J. Chem. Phys*. **1986**, *84*, 2279. (c) Szalewicz, K.; Cole, S. J.; Kolos, W.; Bartlett, R. J. *J. Chem. Phys*. **1988**, *89*, 3662. (d) Gutowski, M.; van Duijneveldt -van de Rijdt, J. G. C. M.; van Lenthe, J. H.; van Duijneveldt, F. B. *J. Chem. Phys*. **1993**, *98*, 4728.
(61) Boys, S. F.; Bernardi, F. *Mol. Phys*. **1970**, *19*, 553.
(62) Dyke, T. R.; Mack, K. M.; Muenter, J. S. *J. Chem. Phys*. **1977**, *66*, 498.
(63) Herbine, P.; Dyke, T. R. *J. Chem. Phys*. **1985**, *83*, 3768.
(64) Gerhards, M.; Schmitt, M.; Kleinermanns, K.; Stahl, W. *J. Chem. Phys*. **1996**, *104*, 967.

(65) Berden, G.; Meerts, W. L.; Schmitt, M.; Kleinermanns, K. *J. Chem. Phys*. **1996**, *104*, 972.
(66) Humphrey, S. J.; Pratt, D. W. *J. Chem. Phys*. **1996**, *104*, 8332.
(67) Stanley, R. J.; Castleman, A. W., Jr. *J. Chem. Phys*. **1991**, *94*, 7744.
(68) Lipert, R. J.; Colson, S. D. *J. Phys. Chem*. **1989**, *93*, 135.
(69) Hartland, G. V.; Henson, B. F.; Venturo, V. A.; Felker, P. M. *J. Phys. Chem*. **1992**, *96*, 1164.
(70) Watanabe, T.; Ebata, T.; Tanabe, S.; Mikami, N. *J. Chem. Phys.* **1996**, *105*, 408.
(71) Michalska, D.; Bienko, D. C.; Abkowicz-Bienko, A. J.; Latajka, Z. *J. Phys. Chem*. **1996**, *100*, 17786.
(72) Ebata, T.; Furukawa, M.; Suzuki, T.; Ito, M. *J. Opt. Soc. Am.* **1990**, *B7*, 1890
(73) (a) Hoke, S. H.; Yang, S. S.; Cooks, R. G.; Hrovat, D. A.; Borden, W. T. *J. Am. Chem. Soc*. **1994**, *116*, 4888. (b) DeFrees D. J.; McIver, R. T., Jr.; Hehre W. J. *J. Am. Chem. Soc*. **1980**, *102*, 3334.
(74) (a) Cunningham, A. J.; Payzant, J. D.; Kebarle, P. *J. Am. Chem. Soc*. **1972**, *94*, 7627. (b) Kebarle, P.; Searles, S. K.; Zolla, A.; Scarborough, J.; Arshadi, M. *J. Am. Chem. Soc.* **1967**, *89*, 6393.
(75) Liu, R.; Morokuma, K.; Mebel, A. M.; Lin, M. C. *J. Phys. Chem*. **1996**, *100*, 9314.
(76) Meot-Ner, M.; Sieck, L. W. *J. Am. Chem. Soc*. **1991**, *113*, 4448.